

PROCEEDINGS OF SPIE

SPIDigitalLibrary.org/conference-proceedings-of-spie

Scientific commissioning of the James Webb Space Telescope

Randy Kimble, Amy DeLisa, Scott Friedman, David Golimowski, Andria Hagedorn, et al.

Randy A. Kimble, Amy S. DeLisa, Scott D. Friedman, David A. Golimowski, Andria Hagedorn, Keith A. Parrish, Carl A. Reis, Jane R. Rigby, Julie M. Van Campen, Lauren R. Wheate, "Scientific commissioning of the James Webb Space Telescope," Proc. SPIE 12180, Space Telescopes and Instrumentation 2022: Optical, Infrared, and Millimeter Wave, 121800Q (27 August 2022); doi: 10.1117/12.2630063

SPIE.

Event: SPIE Astronomical Telescopes + Instrumentation, 2022, Montréal, Québec, Canada

Scientific commissioning of the James Webb Space Telescope

Randy A. Kimble^{*a}, Amy S. DeLisa^{b,a}, Scott D. Friedman^c, David A. Golimowski^c, Andria Hagedorn^d, Keith A. Parrish^a, Carl A. Reis^a, Jane R. Rigby^a, Julie M. VanCampen^a, and Lauren R. Wheate^{e,a}

^aNASA's Goddard Space Flight Center, 8800 Greenbelt Rd., Greenbelt, MD 20771

^bG&N Corporation, 13453 Marble Rock Drive, Chantilly, VA 20151

^cSpace Telescope Science Institute, 3700 San Martin Drive, Baltimore, MD 21218

^dNorthrop Grumman Aerospace Systems, 1 Space Park Blvd., Redondo Beach, CA 90278

^eGeneral Dynamics Mission Systems, 430 National Business Parkway, Suite 200, Annapolis Junction, MD 20701

ABSTRACT

The long-awaited launch of the James Webb Space Telescope on December 25, 2021, initiated a complex commissioning campaign which successfully brought the observatory to readiness for carrying out its scientific observing program by early July, 2022. Commissioning began by bringing online the various spacecraft systems and executing a series of mission-critical deployments. The next few months involved a complex interplay of cooling toward the final cryogenic operating temperatures of the telescope and instruments, aligning the segmented, deployable telescope, bringing online Webb's four scientific instruments (plus Fine Guidance Sensors), and beginning the process of preparing their many powerful observing modes for scientific use. We provide an overview of the process and timeline for executing the commissioning campaign and then focus on its final stages: for each instrument, acquiring the numerous pieces of performance data and carrying out the operational verifications that ultimately led to confirmation of each observing mode's readiness for scientific operations.

Keywords: JWST, Webb, infrared, space telescopes, observatory, OTE, ISIM, commissioning

1. INTRODUCTION

The James Webb Space Telescope (JWST or Webb) is a cryogenic, large-aperture (6.6m diameter), segmented-telescope observatory, covering a wavelength range of 0.6-28 μ m. Webb has been launched, has been deployed to a halo orbit around the Sun-Earth L2 point, and has successfully completed a six-plus-month commissioning campaign. As of early July, 2022, it has entered fully into nominal scientific operations. An overview of the mission and its status is given in this volume by McElwain et al. (2022)¹, and the early technical performance is summarized by Rigby et al. (2022)².

Webb comprises three principal elements:

- 1) the Spacecraft Element (SCE), which houses the usual systems for power, attitude control, communications, command & data handling, propulsion, etc., and also incorporates the large, five-layer sunshield which, when deployed, enables the telescope and instruments to passively cool to their ~40K operating temperatures;
- 2) the Optical Telescope Element (OTE), which consists of a three-mirror anastigmat telescope (with an 18-segment Primary Mirror) and Fine Steering Mirror, along with the composite structures to support those optics and the systems required to deploy them (including the Secondary Mirror Support System, two 3-segment deployable wings for the Primary, and the actuators for deploying and aligning the Primary Mirror Segments and Secondary);
- 3) the Integrated Science Instrument Module (ISIM), which comprises four science instruments (SIs) and the structural, thermal, electronic, and operational systems that support them. The SIs are the Near-Infrared Camera (NIRCam)^{3,4}, the Near-Infrared Spectrograph (NIRSpec)⁵⁻⁸, the Mid-Infrared Instrument (MIRI)^{9,10}, and the Fine Guidance Sensor/Near-Infrared Imager and Slitless Spectrograph (FGS/NIRISS)^{11,12}. Within the last module are both a science channel (NIRISS) and a pair of Fine Guidance Sensor channels that provide pointing error signals on

[*randy.a.kimble@nasa.gov](mailto:randy.a.kimble@nasa.gov); phone 1 301 286-5783

selected guide stars to the attitude control system of the observatory. MIRI has an associated mechanical cryocooler, located primarily in the Spacecraft Element, to drive it to its 6K operating temperature.

The commissioning process was designed to bring all Webb systems to full operational readiness for scientific observing over the course of a nominally six-month-long campaign. Figure 1 shows the baseline commissioning timeline as planned before launch. The schematic sequence initially emphasizes basic spacecraft functionality and the numerous deployments required, then telescope alignment and phasing, and finally the commissioning of the science instruments. There is substantial overlap between the telescope and SI commissioning phases, as the instruments (particularly NIRCam) are brought online to enable the telescope alignment process, and the SIs also execute many of their required activities (such as functionality checks and internal calibrations) before the telescope alignment is complete.

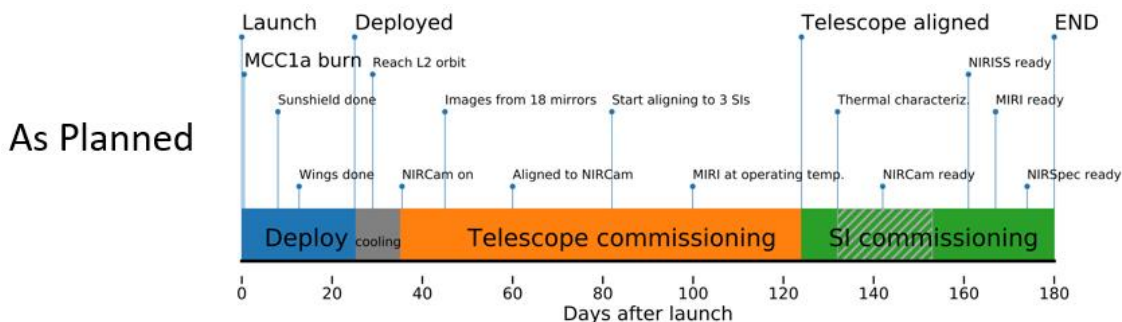


Figure 1. **The pre-flight baseline commissioning timeline**, highlighting the principal phases of commissioning, as well as some noteworthy milestones. “MCC1a” refers to the first mid-course-correction, a time-critical burn that was planned for 12.5 hours after launch. “Wings done” marks the end of the major structural deployments, while “Deployed” indicates that the Primary Mirror segments and Secondary Mirror have also been fully deployed from their launch stops

In Section 2, we give an overview of the as-run commissioning timeline, as well as describing some of the processes utilized to manage the activities. In Section 3, we review the Science Instruments and their capabilities, illustrating the use of some observing modes with examples from Webb’s Early Release Observations, and describe the formal process for certifying the “science readiness” of the modes. In Section 4, we give highlights of the performance of JWST as determined during commissioning. In Section 5, we conclude with the results of commissioning and a summary.

2. COMMISSIONING TIMELINE AND PROCESS

2.1 The overall commissioning timeline

The commissioning of an observatory as complex as JWST required a huge amount of pre-launch planning. Bringing the entire observatory from its stowed launch state to deployed, fully aligned, and ready for science required over 500 distinct activities to be prepared in complete detail before launch. These Commissioning Activity Requests (CARs) were fully defined with all constraints or pre-requisites, success criteria, and deliverable products identified. Many CARs, especially early in the mission, were designed for real-time execution while in radio contact with the observatory. The Mission Operations Center (MOC) at the Space Telescope Science Institute (STScI) in Baltimore was nominally in contact with Webb through the ground stations of the Deep Space Network (DSN) 24 hours a day for the first 4.5 months of the mission, though there were occasional outages for scheduled DSN maintenance or unscheduled problems. Later in the mission, more of the activities were driven by the Onboard Script System (OSS), executing Operating Plans (OPs) uploaded for autonomous, event-driven execution, which carried on whether or not the MOC was in real-time contact, as the DSN coverage was no longer continuous. CARs requiring post-execution data analysis had associated Commissioning Activity Plans (CAPs).

The CARs and CAPs had been thoroughly vetted before launch, over years of development, discussions, and rehearsals. All major CARs concerning deployments and key telescope alignment activities, along with simulated anomalies and contingencies, were executed in pre-launch rehearsals. Activation of spacecraft and instrument systems with real-time commanding was also rehearsed. For the later stages of SI commissioning, when most activities were driven by standard observing templates and the Onboard Script System, only representative CARs were executed during rehearsals. It would not have been practical to rehearse a full six-month timeline!

Based on the years of development and rehearsals, a complete pre-flight commissioning timeline was developed to capture *every* pre-planned activity for the six-month period. This huge effort was accomplished principally by the lead Timeline Coordinators (TLCs) Lauren Wheate, Andria Hagedorn, and David Golimowski. The output was a Commissioning Activities Sequence Timeline (CAST) that captured every command, every configuration change for the first 30-days after launch (through all the deployments and insertion into the L2 halo orbit), as well as a full six-month commissioning timeline with a baseline execution sequence for all the planned CARs, with meticulous documentation of the constraints, pre-requisites, and dependencies.

Those first 30 days after launch were highly dramatic. There were various challenges to be overcome, e.g., learning how best to operate the complex attitude control system (ACS): ACS issues caused multiple safing events, which were all well-handled by the onboard fault management system and the ground operations team, and all benign in terms of the ultimate effects on the flight hardware (we remain on primary systems). Sunshield deployments were interrupted for tuning of the solar array regulators to place the solar panels at appropriate operating points to optimize their efficiency and responsiveness. Deviations from the expected cooldown profile required reshuffling of some temperature-constrained activations, and side-B power had to be added temporarily to one SI's heaters to manage its cooldown properly. The upshot of the first month, however, is that all the critical structural deployments were successfully completed on schedule within the first 14 days, the Primary Mirror Segments and Secondary were deployed smoothly from their launch stops by day 25, and all mid-course corrections en route to the L2 orbit were completed on time, with high precision.

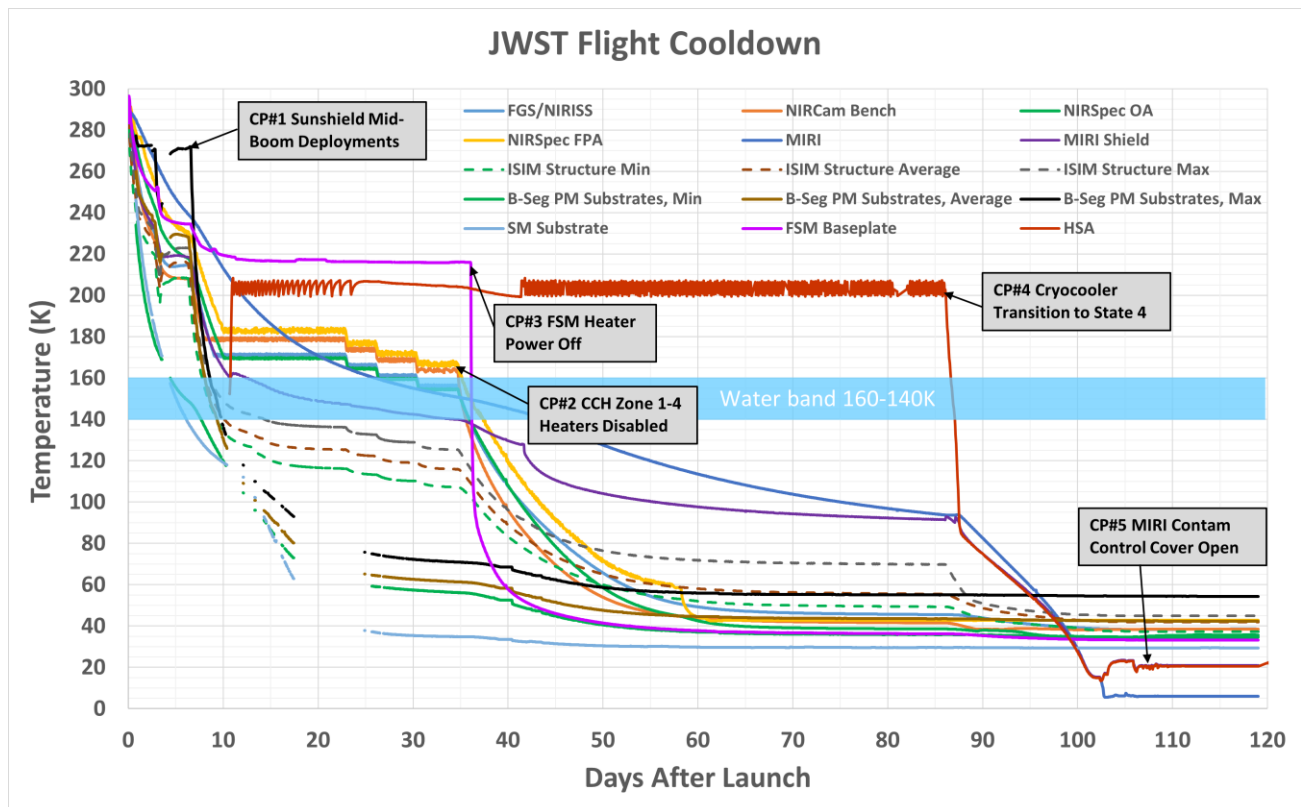


Figure 2. The temperature vs. time for the major JWST systems. The large gaps in mirror temperature collection were during their deployment period. The “Water band” indicated is a roughly defined temperature range in which surfaces transition from being able to desorb water vapor to temperatures where it will stick for long periods. We kept sensitive instrument surfaces above that temperature range until local sources had cooled below 140K. Some legend definitions: B-seg PM = Primary Mirror “B” segments (which are the small hexagonal Primary Mirror Segments that form the vertices of the larger total PM hexagon); SM = Secondary Mirror; FSM = Fine Steering Mirror; HSA = Heat Exchange Stage Assembly (part of the MIRI cryocooler); OA = Optical Assembly; FPA = Focal Plane Assembly; CCH = Contamination Control Heaters. CP = Consent-to-Proceed – those CP text blocks indicate decision points at which the team gathered to confirm readiness for the next planned step; these meetings were scheduled for situations where the next commanded activity would induce a significant (and sometimes irreversible) thermal change in the observatory.

As the payload continued to cool over the following months, the commissioning timeline reflected a complex interplay of managing a safe and contamination-free cooldown, aligning and phasing the telescope (while the structures were still moving due to the cooldown!), and bringing online the various functionalities of the science instruments. Figure 2 summarizes the cooldown of the major systems and illustrates the complexity of this changing thermal environment.

Key takeaways from the cooldown curves include the following. There was an extended hold period in the ~10-to-30-day timeframe during which the near-IR instruments were held above 160K using contamination control heaters while sources of water outgassing (e.g. the ISIM composite structure) cooled around them. When those sources had cooled below outgassing temperatures and the MIRI instrument had passively cooled so that it also would no longer be a source, the instruments were permitted to continue their passive cooldown (with some residual local heater control for particularly sensitive systems). When the instruments had cooled enough to take spectra in the region of the 3.1 μ m water ice feature, the low limits derived on ice absorption on optical surfaces confirmed the success of the contamination control methodology. Most importantly, note that the cooldown to final temperature stability took months – while the near-IR instruments reached temperatures where they could begin useful activities in ~40 to 55 days, the cryocooler did not drive MIRI to its final stable operating temperature until 106 days after launch (L+106d). All these considerations had been captured before flight in a detailed JWST Cooldown Plan, led by Cooldown Working Group lead Amy DeLisa.

Mirror alignment activities began at L+35d when the NIRCcam shortwave detectors (on the <2.5 μ m side of NIRCcam's two dichroic-fed channels) had reached a sufficiently low temperature to begin taking on-sky data. The telescope alignment process dominated the next 60+ days, in a carefully planned, elegant sequence of steps that took the telescope from an initial deployed state in which every star in the field produced 18 separate, out-of-focus images at the telescope's focal plane, to one in which all 18 mirror segments acted together as one smooth optic, fine-phased so as to yield diffraction-limited performance at a wavelength of 1.1 μ m vs. the requirement of 2.0 μ m. This spectacularly successful process is described in several papers in these proceedings^{1,13-15}, so we do not elaborate further here. The final two months of commissioning then focused on instrument commissioning and the execution of a highly successful thermal stability test¹.

2.2 Management and execution of JWST commissioning

Though we have noted the development of a full six-month pre-launch baseline commissioning timeline, there was of course no expectation that such an extended sequence would run as written. The mirror alignment process alone had myriad alternate paths and uncertain numbers of iterations for key steps, which would be executed or not depending on the accuracy of the previous iteration. When the response to anomalies, deviations of the cooldown from the pre-flight model, failed observations, or the state of necessary analyses are added in, it is clear that great flexibility was needed.

One invaluable tool in managing the commissioning flow was a daily meeting called the JWST Daily Briefing (JDB). The purpose of this meeting was to provide the members of the commissioning team with status of key systems and activities, to replan the timeline sequence according to the real-time needs, and to share performance results as those were obtained. The meeting was chaired initially by one of the Mission Operations Managers, Carl Reis, but as the commissioning activities shifted from basic functionality to alignment and scientific performance, the meeting for most of the commissioning period was chaired by STScI's JWST Commissioning Scientist, Scott Friedman.

The JDB was held seven days a week for most of commissioning, with Sundays off as operations became more routine (off, that is, in terms of holding this particular meeting – not in terms of continuing with the commissioning activities!). Topics of discussion included:

- General announcements
- Timeline progress – TLC review of recently completed activities, noting upcoming activities and the state of their pre-requisites, *replanning discussion for the coming few days if needed*, highlighting upcoming targets
- Facilities status
- Thermal status
- Telescope alignment progress/status
- Science instrument status from a state-of-health, anomalies standpoint
- Pointing performance (in particular Fine Guiding results, as that system came online)
- Ground systems status
- Onboard Script System status and updates

- JSOCOPS ticket status (this topic will be described below)
- Science instrument commissioning progress and performance results, issues

As the cooldown was completed, or status became routine (e.g. for facilities), topics were reported only as needed. **The discussions of any necessary timeline adjustments and then the SI performance results became the focus for the final months of commissioning.**

When possible, near-term adjustments to the timeline were adjudicated with the TLCs at the JDB. There were of course also mechanisms for necessary real-time changes between these meetings – these were coordinated among the relevant systems, the Mission Operations Manager (MOM), and the TLCs, with cognizance and approvals for all parties who needed to be involved.

A broader perspective on upcoming activities was provided at a Weekly Replan Meeting, led by the lead TLC, Lauren Wheate. At these meetings, a look-ahead at the coming 7-10 days of activities was provided, identifying the planned sequence of CARs, as well as any DSN outages or special activities like station-keeping maneuvers (for maintaining the L2 orbit) or momentum unloads. The focus of these presentations was a “waterfall” diagram of upcoming activities; a portion of one of these is excerpted in Figure 3.

The JDBs and the Weekly Replan meetings proved to be effective means for keeping the large Webb commissioning on the same page as the complex process of bringing the observatory to readiness for nominal operations proceeded.

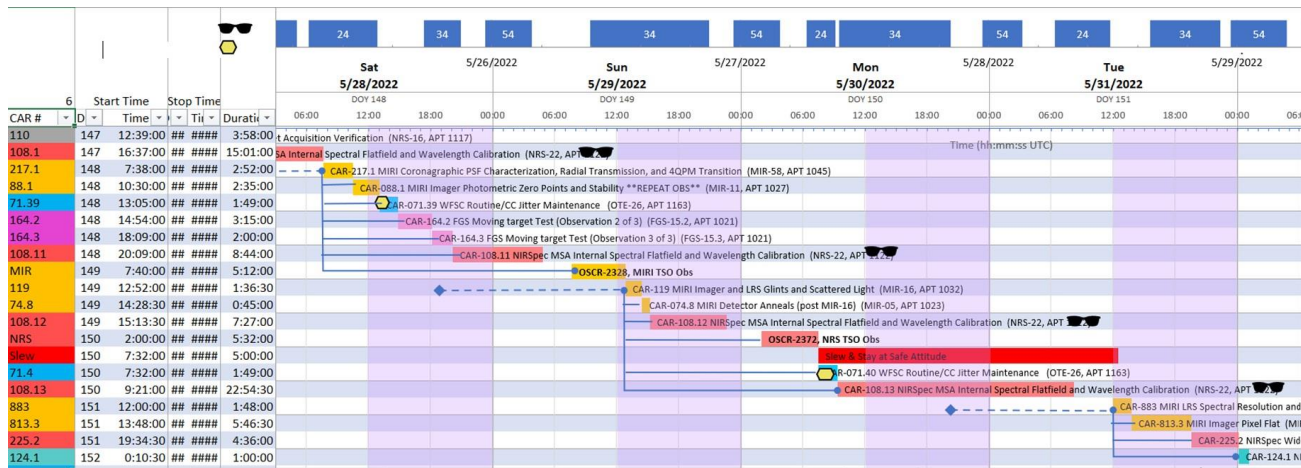


Figure 3. Sample waterfall diagram of upcoming activities, as presented at a JWST Weekly Replan meeting.

For a system as complex and valuable as JWST, it was of course essential that formal processes be used to control and document the commissioning activities. A record of the progress of JWST commissioning was established through the use of electronic files of various types in the MOC. These included TSRs, OSCRs, FSCRs, and JSOCOPS tickets, whose definitions and purposes we describe briefly here:

- **Timeline Scheduling Request (TSR):** All expected commissioning activities were in the baseline plan prior to launch. To ensure that no OP-driven activity was executed until the responsible teams were ready, the OP was not prepared for upload to the observatory until the team filed a TSR. This guaranteed that the SI teams, the TLCs, and others agreed that all prerequisites for that activity had been met.
- **Operations Schedule Change Request (OSCR):** Changes to the baseline plan were inevitable and anticipated, so OSCRs were established to deal with them. A variety of discipline representatives and the MOM had to approve each OSCR. Once an OSCR was approved, the TLCs added the activity to the schedule. TSRs and OSCRs were typically filed 1-3 days prior to execution, but they were implemented on shorter turnarounds when required.
- **File System Change Request (FSCR):** The flight software commands, configuration tables, standard-operating procedures, and telemetry display pages for all JWST subsystems are contained within the Flight Operations Project Reference Database (PRD). To add or update any files in the Flight Operations System (FOS) prior to formal

release of a new PRD required the submission, review, and approval of a FSCR. All flight products associated with a FSCR had to be vetted on a spacecraft simulator before the FSCR could be approved and the products transferred to the FOS.

- TSRs, OSCRs, and FSCRs were managed on a JIRA system installed on and limited to the FOS. This system allowed for timely notification of those required to approve each request, a means of tracking the status of each approval, and a searchable, permanent record of the requests.
- **JWST Science & Operations Center Operations (JSOCOPS) tickets:** Making changes to either the flight or ground system also requires careful coordination among multiple subsystems. Consequently, a second JIRA system outside the FOS was used to manage and record these changes via JSOCOPS tickets, which typically contain a detailed list of the activities required to implement the change as well as a list of the subsystems who contribute to the task. Only when each participating subsystem approves the ticket, signifying that their task is complete, is the ticket closed. Once again, the JIRA system provides a convenient electronic record of changes.

2.3 Summary of the as-run commissioning timeline

Having given a flavor for the overall process and plan for commissioning JWST, we summarize here how it all came out. A schematic of the **as-run** timeline is presented in Figure 4: in it, we highlight a number of noteworthy steps along the path to the final telescope alignment, as well as some highlights along the path to the scientific commissioning of the various SI observing modes.

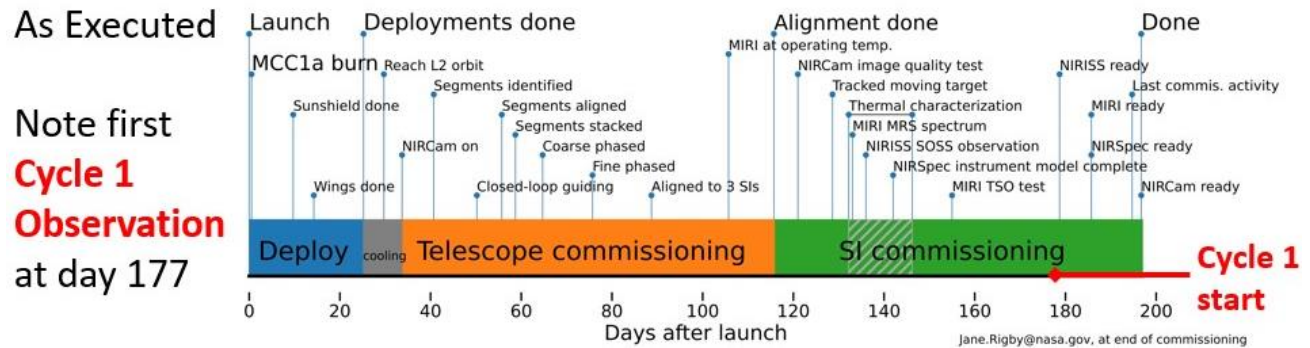


Figure 4. The actual as-run timeline for JWST commissioning. It was not fully completed until L+197d, but the final weeks of commissioning activities were interleaved with Cycle 1 observing, which began at L+177d.

Figure 4 shows a final completion date for commissioning of L+197d, vs. a target of L+180d. The final onboard commissioning activity had run a few days before L+197d. For a system of such complexity this was remarkably close to the baseline plan. Even that modest additional duration was not purely commissioning time. Two of the SI observing modes needed final adjustments that required iterations of software or database updates, observations, and analyses, with some days in between. Accordingly, available time between those final commissioning activities was filled with the first observations of JWST Cycle 1, for modes that were already fully available for use.

The very small exceedance of the baseline plan should not be taken to imply that there were no challenges, however! Numerous difficulties had to be surmounted. There were half a dozen safing events as the team learned to deal with the flight behaviors of the complex systems. These required careful analysis and meticulous recovery, but fortunately in no cases represented actual hardware failure of the primary systems. Unplanned DSN outages posed delays. Pointing system control loop parameters had to be empirically tuned. Flight software bugs were discovered and corrected. Failed observations were rescheduled and repeated. Unexpected behaviors were investigated with new diagnostic observations.

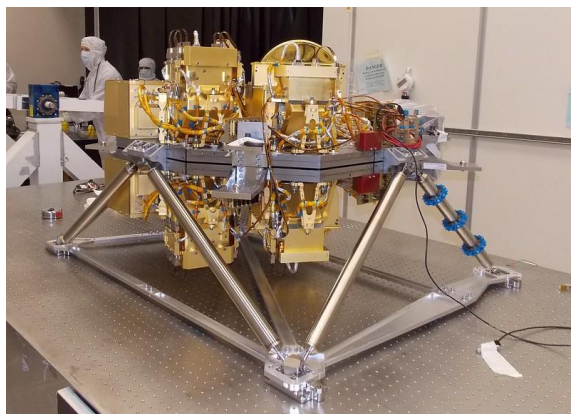
Time *savings* vs. the baseline plan came principally in two areas. The mirror alignment and phasing process went beautifully^{1,13-15}. Sufficiently high precision was obtained in the wavefront measurements and mirror adjustments in various stages of the alignment process that planned additional iterations were not required. Later, a thermal stability test planned for a two-week duration was truncated early, because the system settled more quickly after a hot to cold slew than had been predicted (the thermal time constant of the mirror backplane structure was shorter than modeled).

The result of all the puts and takes was a commissioning duration in excellent agreement with the baseline plan. As indicated, the activities culminated with the commissioning of the science instruments, and we turn our attention there for the remainder of this paper.

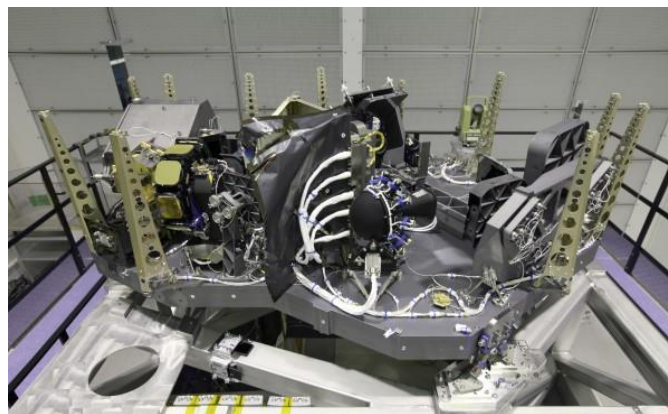
3. SCIENCE INSTRUMENT COMMISSIONING

3.1 The JWST instruments and their observing modes

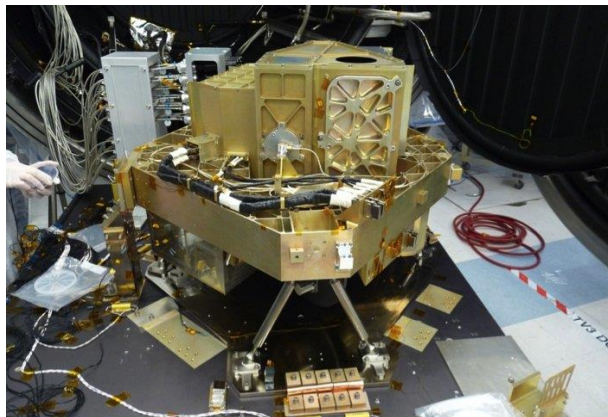
The focus of commissioning in the final months was bringing to observational readiness Webb's powerful suite of instruments. As described above, there are three near-infrared instruments, which each cover a wavelength range of 0.6-5.0 μm – the Near-Infrared Camera (NIRCam), the Near-Infrared Spectrograph (NIRSpec), and Near-Infrared Imager and Slitless Spectrograph (NIRISS) – and the Mid-Infrared Instrument (MIRI), which covers from 5.0-28 μm . NIRISS is packaged with another key Webb element, the two-channel Fine Guidance Sensor (FGS), a major part of the Attitude Control System control loop that stabilizes JWST pointing to the milli-arcsec level. Photos of the instruments are shown in Figure 5, along with the names of their Principal Investigators and principal organizational developers.



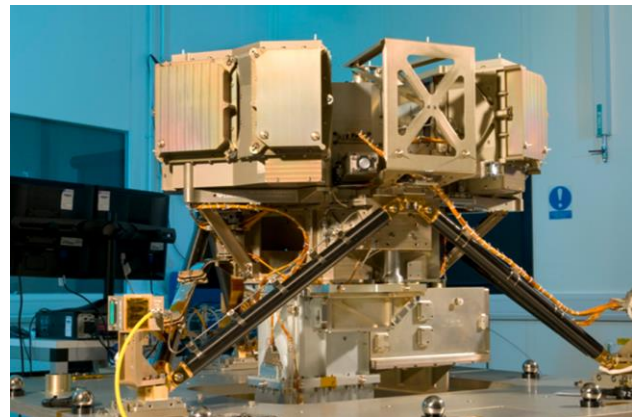
NIRCam -- PI: Marcia Rieke
University of Arizona, Lockheed Martin



NIRSpec – PI: Pierre Ferruit
ESA, Airbus Defence and Space



NIRISS/FGS -- PI: René Doyon
CSA, Honeywell



MIRI – PIs: Gillian Wright & George Rieke
European Consortium, ESA, RAL, JPL, U. of Arizona

Figure 5. The Science Instruments (SIs) of JWST, with their Principal Investigators and developers.

It is important to note that *the instrument teams themselves had the major responsibility for the commissioning of their instruments*; they defined the Commissioning Activity Requests and Commissioning Analysis Plans and executed them over six and a half grueling months of flight activities. All teams had many important contributing members, but we highlight the commissioning leads for each instrument here: NIRCam (John Stansberry, Martha Boyer); NIRSpec

(Torsten Böker, Stephan Birkmann, Charles Proffitt, Tim Rawle), NIRISS (André Martel, Paul Goudfrooij, Stephanie LaMassa), MIRI (Alistair Glasse, Sarah Kendrew, Alberto Noriega-Crespo, Macarena Garcia Marin), and FGS (Begoña Vila, Ed Nelan, Pierre Chayer). Several papers documenting the teams’ results can be found in these proceedings¹⁶⁻²⁴.

Collectively, these instruments offer an extremely powerful set of observing modes: 17 in all, listed in Table 1. Some are relatively “standard” and familiar to Hubble users, but offered with unprecedented sensitivity and wavelength coverage: e.g. imaging, long-slit spectroscopy, Lyot coronagraphy with occulting spots – while other capabilities are being offered for the first time in a space facility at these wavelengths: multi-object spectroscopy with a programmable shutter array, integral field spectroscopy, and high-contrast imaging through the use of aperture masking interferometry (NIRISS) or 4-quadrant phase masks (4QPM, MIRI).

Table 1. The observing modes of JWST

NIRCam

- Imaging
- Wide Field Slitless Spectroscopy
- Time Series – Imaging
- Time Series – Grism
- Coronagraphic Imaging

NIRISS

Wide Field Slitless Spectroscopy

- Single Object Slitless Spectroscopy
- Aperture Masking Interferometry
- Imaging (parallel only)

NIRSpec

- Multi-Object Spectroscopy
- Fixed Slit Spectroscopy
- Integral Field Unit Spectroscopy
- Bright Object Time Series

MIRI

Imaging

- Low Resolution Spectroscopy
- Medium Resolution Spectroscopy
- Coronagraphic Imaging

As a preview of the outcome of JWST commissioning, the Webb Early Release Observations offer tantalizing glimpses of the capabilities of the observatory – we include some here to demonstrate some of the modes from Table 1, but we urge any readers who haven’t explored these images already to view them in their full, high-resolution glory online.



Figure 6. Examples of Webb imaging. (left) NIRCam imaging of the SMACS 0723-73 field, which represents the deepest IR image ever taken to that date, accomplished with a total exposure time of only 12.5 hrs. Besides the sensitivity increase, Webb’s large mirror diameter offers a factor of $6.6\text{m}/2.4\text{m} = 2.7\text{x}$ resolution advantage at comparable wavelengths vs. Hubble. (right) The comparison is even more stark vs. the highly successful, but small (only 0.85m-diameter) Spitzer telescope; the Webb resolution gain vs. Spitzer, shown here at 8um wavelengths, is dramatic.

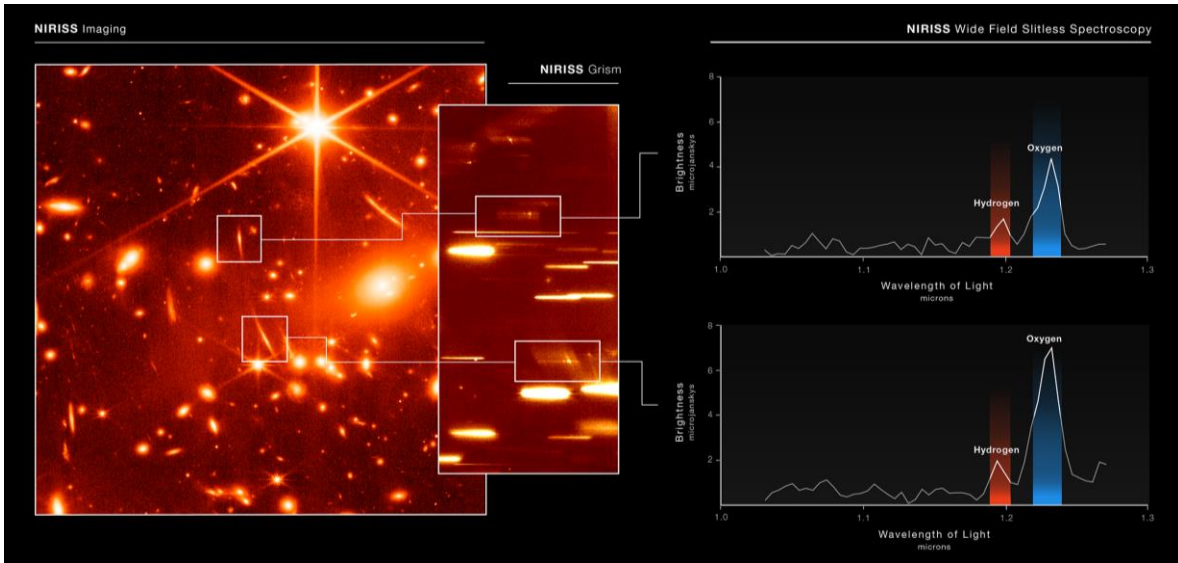


Figure 7. The power of Wide Field Slitless Spectroscopy is demonstrated with these NIRISS grism spectra of two lensed arcs in the SMACS 0723-73 field. The common redshifts of the observed spectral lines confirm that these arcs are lensed images of the same background galaxy.

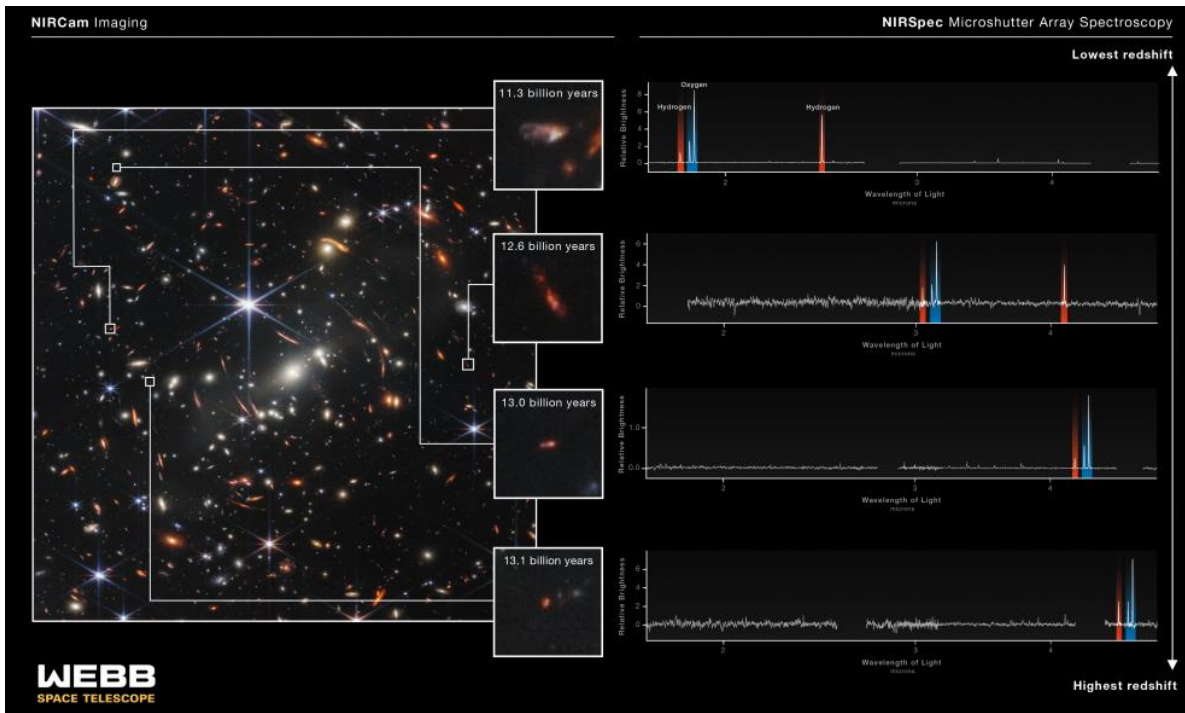


Figure 8. The greatest sensitivity for spectroscopic observing with Webb is achieved with the Multi-Object Spectroscopy observing mode offered by NIRSpec – the first long-term use of such a capability in space – offered by a programmable micro-shutter array²⁴⁻²⁶. With such a capability, spectral overlap of sources can be avoided, and the bright zodiacal background in the infrared is minimized by opening only shutters required to form narrow slits across the desired targets. This capability can be applied to >200 targets in low-resolution prism mode and ~60 targets in medium or high-resolution grating modes. Here, multiple slitlets have been opened at the positions of interesting targets in the SMACS 0723-73 field. The resulting spectra capture a broad range of redshifts, out to a z of 8.5.

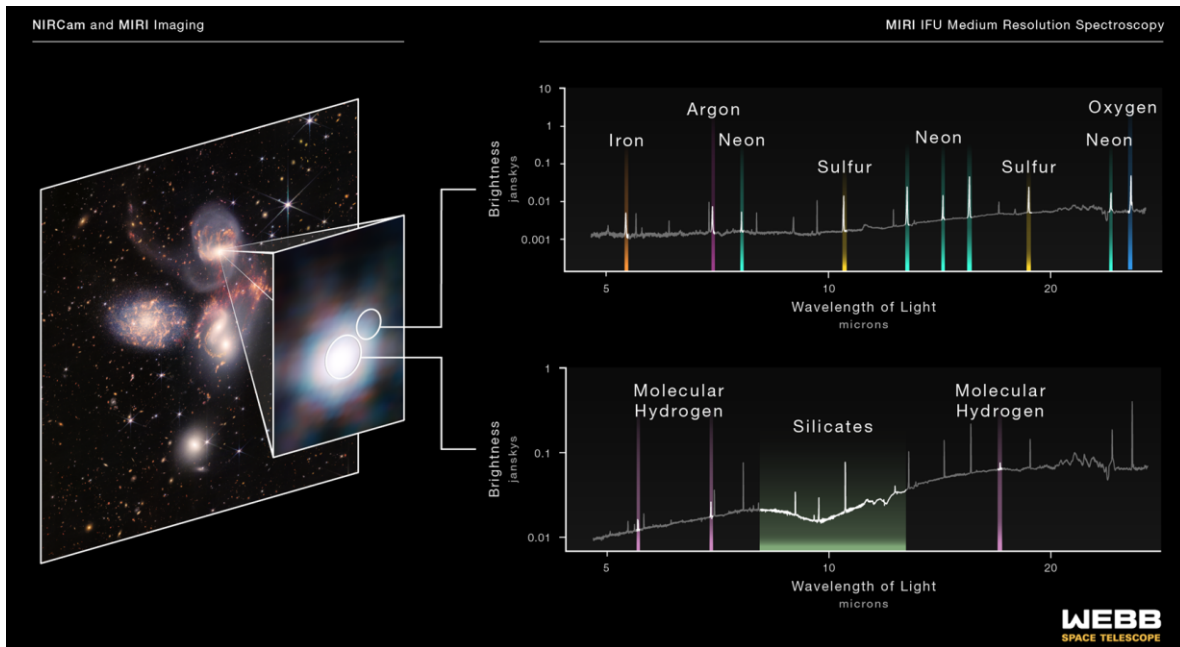


Figure 9. Webb’s integral field capability extends over the full 0.6-28 μ m range, with the use of image slicers in the NIRSpec and MIRI instruments.

Here the capability for obtaining spectral data over a several arcsecond area in each dimension is illustrated for the study of the surroundings of the central black hole in one of the galaxies in Stephan’s Quintet. The resulting data cube is sliced (top) to show the MIRI spectra in two distinct spatial regions around the black hole. The NIRSpec data cube is sliced (at left) to show the distinct spatial maps of different emission lines in the region.

These are brief examples of a few of Webb’s observing capabilities. The novel capabilities for time series observations and for high-contrast imaging will be discussed further in Section 4.2.

3.2 The goals of SI commissioning

For the instruments, the goal of commissioning was to bring them to a state of readiness for use in Webb’s selected Cycle 1 observing program. Commissioning thus sought to characterize the performance and operational readiness of each observing mode well enough to know how to take “science-quality” data with it. Accordingly, the SI commissioning tasks included:

- Exercising the entire process of planning, executing, and archiving observations – from the observation planning templates (in the Astronomer’s Proposal Tool [APT]), to the Planning & Scheduling system used to construct

Observing Plans, to the Onboard Script System that executes the Observing Plan, to downlinking, pipeline processing and archiving the resulting data.

- Exercising all major observing features of each observing mode – e.g. dithers, mosaics, target acquisition, subarrays – though of course not with all possible parameter choices.
- Getting a reasonable *start* on the calibration of the modes, sufficient to understand how to take quality data of appropriate signal-to-noise. It is recognized, however, that calibrations will be refined through the planned Cycle 1 calibration program and further through the life of the mission. *Some* calibrations must be precise from the start – e.g., astrometric calibrations of the positions of slits, coronagraphic nulls, or occulting spots – but others will be refined later.
- Quantitatively assessing the performance of the modes against a variety of metrics.
- Assessing, in at least a preliminary way, the effectiveness of the standard data-processing pipeline for each mode. Observed defects in the pipelines were documented when observed and prioritized for correction; however, it is not the case that the pipelines had to be perfect before effective *observing* with a mode could begin. The pipelines will also evolve over the course of the mission.

3.3 The mode readiness process

After the goals listed above had been accomplished, the end game of commissioning was to formally certify each SI observing mode as being “ready for Cycle 1 science”. For each mode, we had a variety of quantitative performance metrics, agreed upon by the relevant stakeholders. These had been documented long before launch in an internal project memo by the STScI and NASA Commissioning Scientists (Scott Friedman and Randy Kimble, respectively).

For imaging, the metrics included image quality, sensitivity (limiting flux at a given S/N in a given observing time), astrometric precision, ghosts, subarray vs. full-frame flux calibration, and stability. For spectroscopy, the metrics added the quality of the dispersion solutions and the determination of the relative spectral response. It was recognized that the quantitative criteria could not be applied rigidly as “go/no-go” criteria – many performance parameters are beyond one’s control once a payload is in space. Nonetheless, they provided a benchmark level for comparison. For metrics like target acquisition accuracy, underperformance vs. the criteria/expectations led in a couple of cases to the discovery of algorithm errors in the onboard scripts, which were appropriately corrected.

For time series observations and high-contrast imaging, it was expected that the performance of the modes would improve over time, as various instabilities and how to mitigate them were recognized (for time series observations) or as suitable PSF libraries were accumulated. Accordingly, readiness criteria for those modes were set at relatively modest levels – commissioning performance comfortably exceeded those pre-launch expectations, as will be described below.

The readiness process for each mode culminated with a detailed presentation by the relevant instrument team of everything they had learned over the course of commissioning regarding the performance of the mode, the thoroughness of the exercising of observing templates, the significance of any residual anomalies, the performance of the data processing pipeline, and anything else that upcoming observers would need to know to use the mode properly and effectively. At the end of this presentation to scientific peers within the Webb program, the official certification of readiness of the mode for Cycle 1 use was formal approval by NASA’s Senior Project Scientist for Webb, John Mather, and by STScI Director Ken Sembach.

4. PERFORMANCE HIGHLIGHTS

In this forum, we will not try to capture everything that came out of the commissioning program regarding the outstanding scientific performance that Webb demonstrated during commissioning. The paper “Characterization of JWST science performance from commissioning” by Rigby et al. (2022)² offers the most comprehensive early assessment of Webb’s performance; a special issue of Webb papers planned for Publications of the Astronomical Society of the Pacific in late 2022 will provide further details. We will, however, present some highlights.

The image quality of Webb’s segmented-primary-mirror telescope, deployed and aligned in space, is outstanding, far exceeding requirements. With a requirement for diffraction-limited performance at 2 μ m, Webb demonstrated diffraction-limited performance to at least 1.1 μ m, with usefully high Strehl (0.6) all the way to 0.7 μ m. This spectacular performance is described in detail in Rigby et al. (2022)² and in several papers from this conference^{1,13-15}. This is achieved despite the effects of a micro-meteoroid impact that was larger than had been expected for so early in the mission; see Rigby et al. (2022)² for further discussion of micro-meteoroid impacts and potential mitigations.

4.1 Sensitivity

Of the performance criteria against which the modes were judged, the one of probably the greatest scientific significance is sensitivity – how faint can Webb go in a given observing time? The performance for this parameter is outstanding as well, so we touch on that topic here.

The minimum detectable flux in a given observation can be derived (in the standard S/N equation), from four principal parameters: throughput, image quality (encircled energy), background intensity, and detector noise (read noise, dark current, glow, residual cosmic rays). The image quality, as already noted, surpasses requirements for wavefront error and Strehl, and hence also for encircled energy. Smith et al. (2022)²⁷ in this conference describe measurements of the sky, stray light, and observatory thermal background which indicate that the backgrounds are below (in the near-IR) or at (for the mid-IR wavelengths dominated by the Observatory's self-emission) the levels predicted by the JWST Background Model used by the Exposure Time Calculator (ETC). Detector noise is in close agreement with the noise levels observed on the ground, with small increases attributed to residual cosmic ray signals not removed by the pipeline. The differences are small, and we note that no tuning of the SIDECAR ASICs used for the near-IR detector readouts was required in flight. Many Webb observing modes are *background-limited*, so this small increase in detector noise has negligible effect on sensitivity. For NIRSpec, most of the spectroscopy modes have very low sky background and are hence *detector-limited*; for this case, however, the ETC explicitly includes an estimate of the effects of residual cosmic rays on the noise level – this estimate was found to be conservative vs. the observed flight performance¹⁶.

With those three parameters found to be good or neutral vs. pre-flight expectations, what about throughput? The news here is also excellent: over most wavelengths, for most modes, the measured throughput based on observations of flux standard stars was found to be higher than assumed by the ETC. A few % of this exceedance comes from the excellent performance of the contamination control team on the ground – their final pre-launch measurements indicated PAC (percent area coverage) and molecular contamination levels significantly below allocations. Most of the ten to tens of % exceedance typically seen appears to have come, however, from conservative pre-flight assumptions regarding the instrument throughputs. Examples of the observed throughput vs. pre-flight estimates are shown in Figures 10-12.

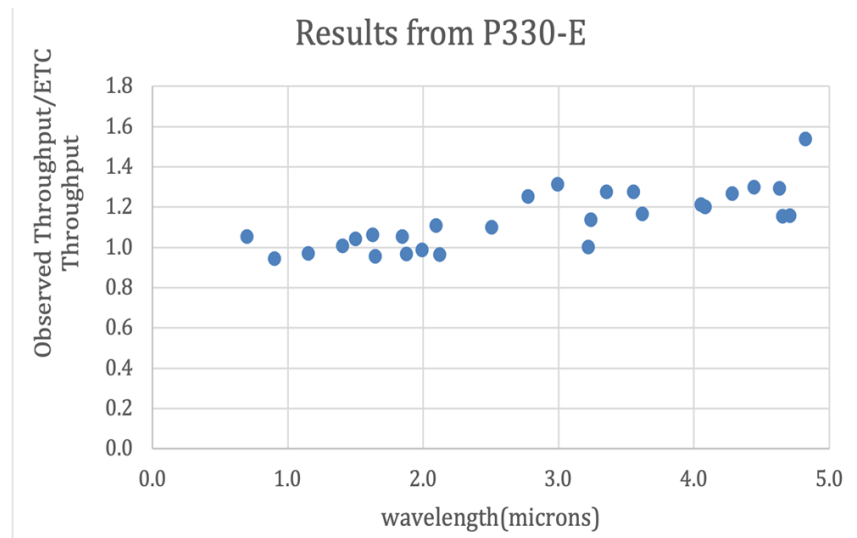


Figure 10. For NIRCcam imaging, the ratio of the observed throughput of the telescope + NIRCcam divided by the pre-flight assumptions incorporated in the ETC is shown for the observation of P330-E, a spectrophotometric standard star. For the shortwave channel of NIRCcam, the ratio is 1 within uncertainties, but the longwave channel throughput is significantly higher than had been assumed. Figure from Rigby et al, (2022)², courtesy of the NIRCcam team.

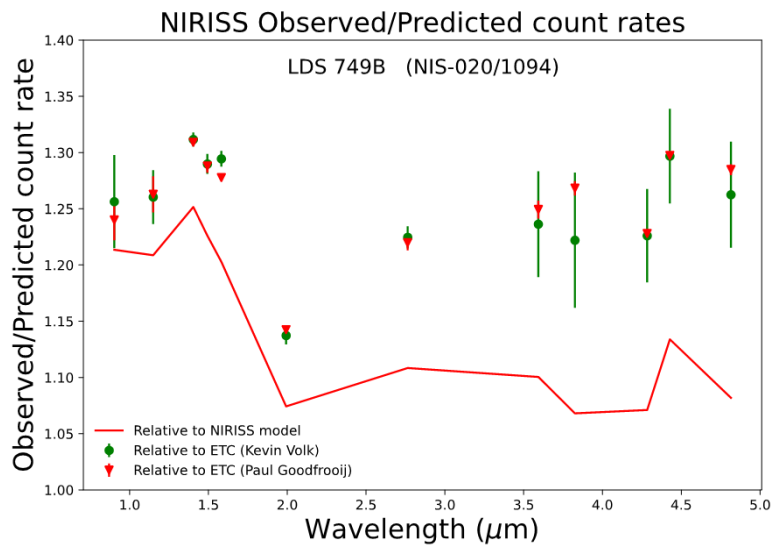


Figure 11. Similarly, for NIRISS, the observed instrument + telescope throughput is higher than that assumed in the ETC, typically by 10-25%. Figure from Rigby et al, (2022)², courtesy of the NIRISS team.

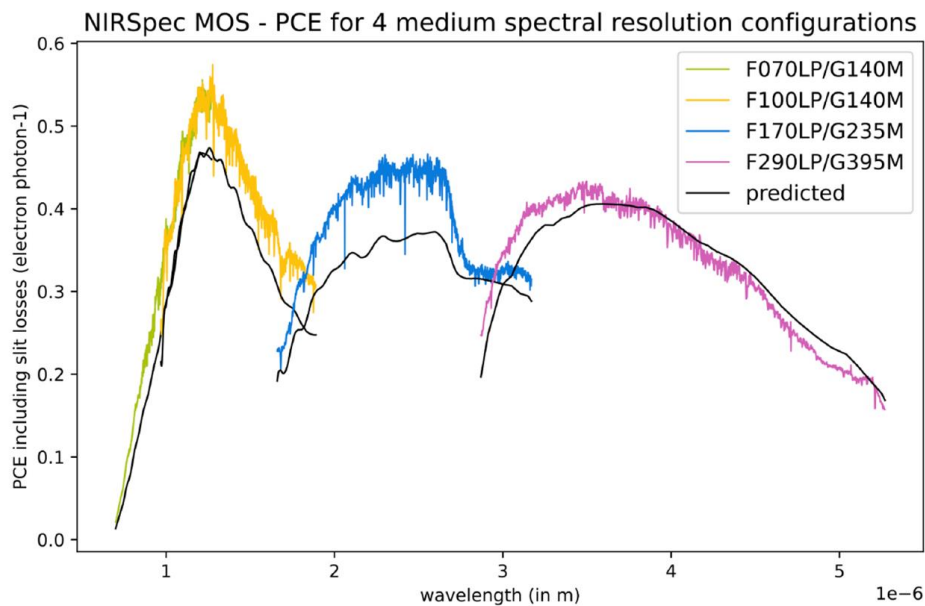


Figure 12. For NIRSpec, the observed throughput is higher than expectations over most of the wavelength range, with small deficits (<10%) at the longer wavelength end of the band^{17,18}. The effective throughput of NIRSpec is further improved for most observations by the excellent image quality delivered to the instrument, which results in smaller slit losses, especially at shorter wavelengths. Figure from Rigby et al (2022)², courtesy of the NIRSpec team.

MIRI throughput is also observed to be higher than expected, though the exact amount of increase depends on the final gain calibration for the instrument.

As an example of the excellent sensitivity performance, Table 2 presents the currently estimated NIRCам throughput vs. pre-flight expectations.

Table 2. NIRCam sensitivity predictions, as estimated from commissioning performance, vs. ETC expectations. Table from Rigby et al. (2022)², courtesy of the NIRCam team.

Wavelength (μm)	2	3.5
Requirement (nJy)	11.4	13.8
ETC prediction (nJy)	10	14.1
Actual (nJy)	7.3	8.8

These improvements vs. expectations, of 25-40%, are typical of what can be expected at many wavelengths and in many modes of the Observatory. The ETC will be updated before the Cycle 2 Call for Proposals to capture these significant performance exceedances over expectations.

4.2 Time series observations

As noted above, in setting the readiness criteria for the time series observing modes of Webb, it was considered prudent to make the goals modest, with the anticipation that the community would “learn by doing” as has been the case for such uses of previous facilities (e.g. exoplanet transit grism spectroscopy with HST/Wide Field Camera 3). Hence, a criterion was set to demonstrate the performance of time series observing with a noise level of 100ppm (parts per million) at a spectral resolving power of 100 for the near-IR instruments and 50 for MIRI. In fact, the stability of the system was found overall to be excellent, and these levels were readily achieved.

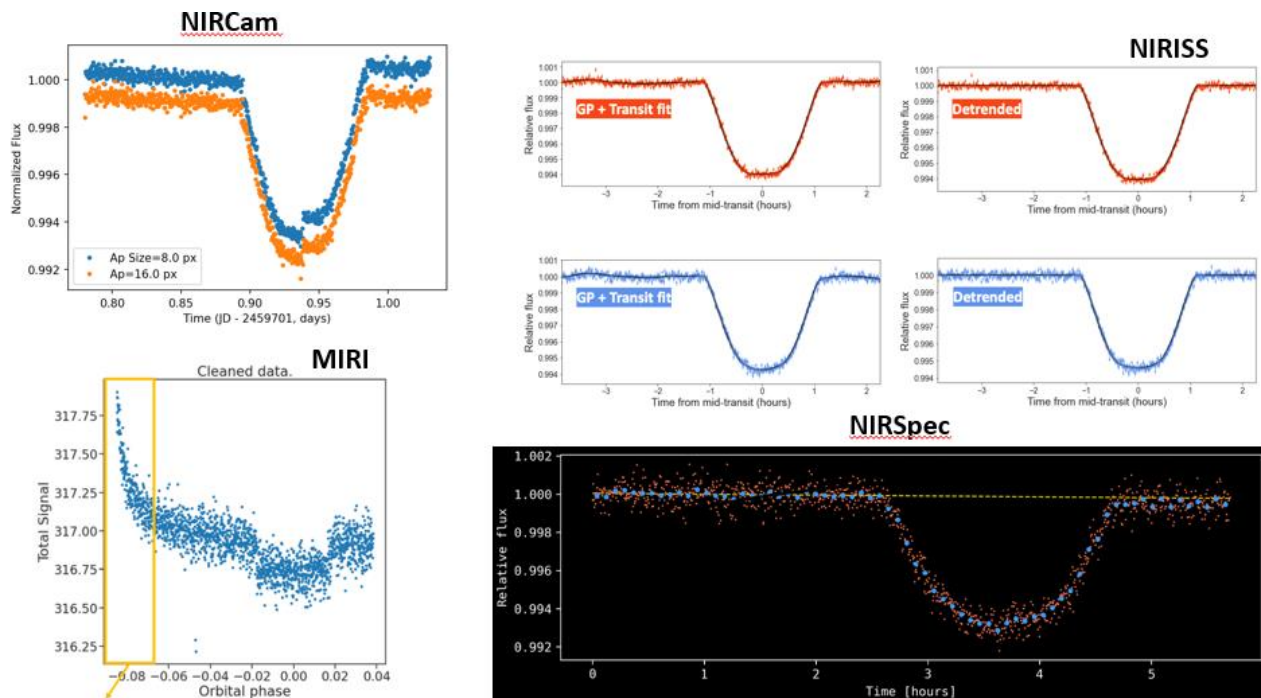


Figure 13. The broadband light curves obtained in the commissioning demonstrations of time series observations for the transiting exoplanets HAT-P-14 (NIRCam, NIRSpec, and NIRISS) and L168-9b (MIRI). After brief stabilization periods, the stability was found to be excellent, suitable detrending was straightforward, and high-precision transit depths at the target resolutions were obtained (see text). The jump observed in the NIRCam observation reflected a so-called “tilt event” in one of the primary mirror segments during the transit (see discussion in Rigby et al. (2022)²), which was easily recognized and removed from the time series. Figures courtesy of the respective instrument teams.

Both demonstration targets were high-mass exoplanets having atmospheres with small scale heights, expected to show spectrally featureless transit depths, to high precision. That is indeed what was recovered from the transit spectra. From single transits of HAT-P-14, NIRCcam derived a transit depth with a precision of 91ppm (with a 55ppm photon-noise floor), NIRISS showed a scatter of 92ppm in the first order spectrum and 85ppm in the second order spectrum), while NIRSpec obtained precisions of 50ppm and 66ppm in the spectral regions of its two detectors, all at spectral resolving power of ~ 100 . MIRI demonstrated a precision of 50ppm at a spectral resolving power of 50 on L168-9b.

On the other hand, for a planet with a more interesting atmosphere – Wasp-96b – the Early Release Observation using the NIRISS Single Object Slitless Spectroscopy demonstrated high S/N detection of multiple spectral features of water vapor in the planet’s atmosphere (Figure 14).

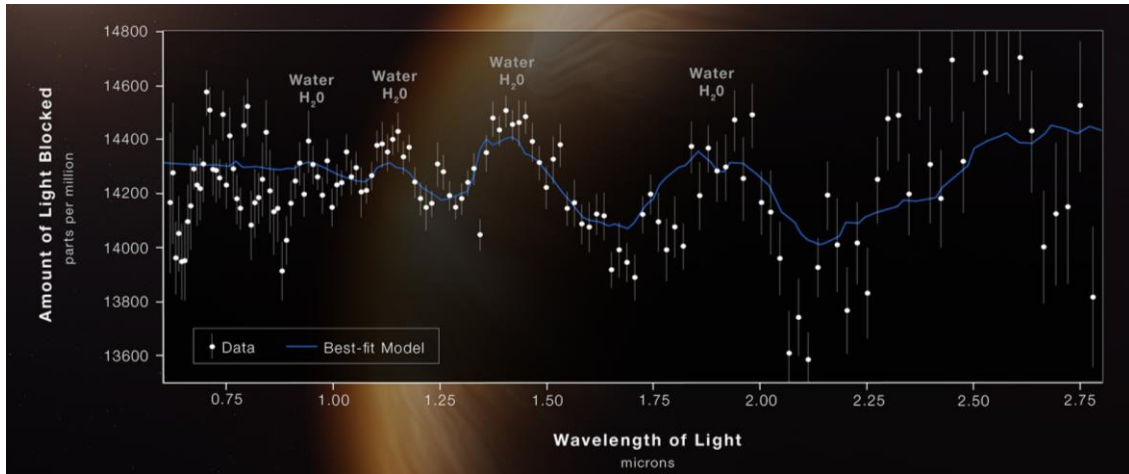
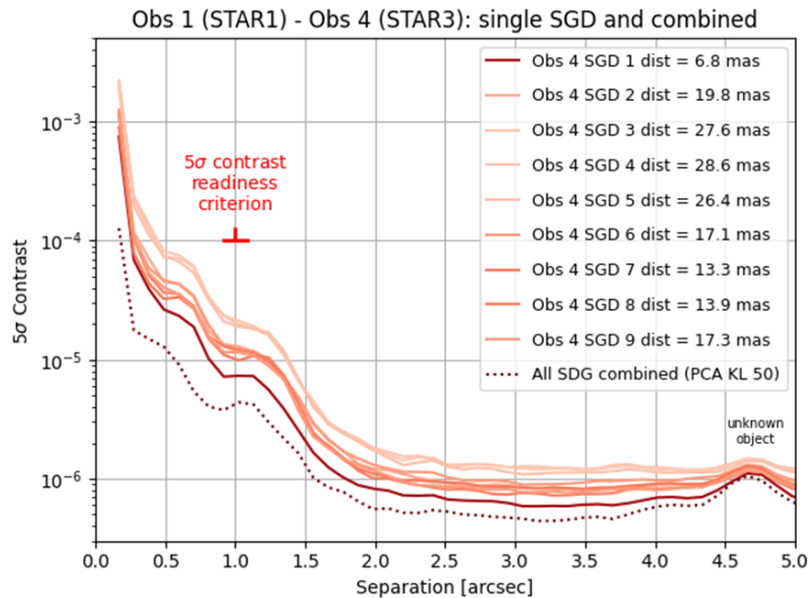


Figure 14. NIRISS Single Object Slitless Spectrum of the hot, steamy atmosphere of the exoplanet Wasp-96b. The amount of light blocked by the exoplanet atmosphere is plotted, so the peaks correspond to strong absorption.

4.3 High-contrast imaging

The high-contrast imaging modes also performed very well in their commissioning checkouts. The readiness criterion for contrast with NIRCcam coronagraphy was 10^{-4} at a one arcsecond separation, comfortably exceeded in commissioning²², as demonstrated in Figure 15.

Figure 15. NIRCcam coronagraphy demonstration at a wavelength of $3.35\mu\text{m}$. The PSF-subtracted contrast curves using each position of the (recommended) 9-point Small Grid Dither pattern individually are shown, along with the higher contrast achieved by combining all dithers with Principal Component Analysis and Karhunen-Loeve processing.



MIRI mode readiness criteria for high-contrast imaging were also comfortably exceeded during commissioning. The MIRI 4QPM coronagraphs needed to demonstrate a raw contrast better than 2400 (pre-PSF subtraction), and the Lyot coronagraph needed to demonstrate a raw contrast better than 1200, all at an angular separation between objects of $6\lambda/D$. (Note, MIRI coronagraph contrasts listed here use the reciprocal definition compared to the NIRCcam coronagraph section). The contrast seen in the 1140C 4QPM is better than requirement-level expectations at all separations where photon noise does not dominate. Table 3 summarizes the raw contrast of all MIRI coronagraphs.

Table 3: Contrast and rejection ratios for all MIRI coronagraphs, as measured during commissioning. Table from Rigby et al. (2022)², courtesy of the MIRI team.

Coronagraph	MASK1065	MASK1140	MASK1550	MASKLYOT
Raw contrast ($6\lambda/D$)	10,570 ± 240	12,700 ± 330	14,700 ± 480	10,260
Rejection ($3\lambda/D$)	108.1 ± 8.8	108.8 ± 5.6	135.8 ± 7.1	233.5
Star subtraction (3σ at $6\lambda/D$)	61,800	47,300	24,100	N/A

The final high-contrast mode assessed during commissioning was the Aperture Masking Interferometry mode of NIRISS, which utilizes a non-redundant mask to achieve moderately high-contrast performance at smaller inner working angles than the Lyot coronagraphs. The demonstration was made on AB Dor C, with a separation of 0.33 arcsec and a delta magnitude of ~ 4.5 . The observations readily detected the companion, at high S/N, and the noise properties indicated a contrast capability for those observations of 6.5-7 magnitudes to an inner working angle of <0.15 arcsec (Figure 16.)

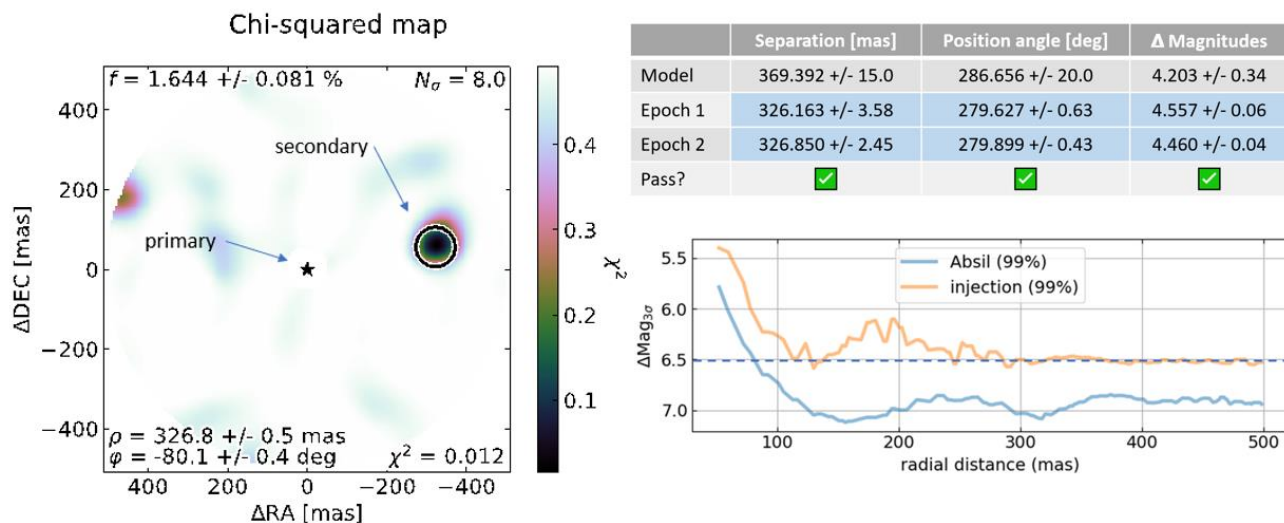


Figure 16. Summary of the NIRISS Aperture Masking Interferometry observation of AB Dor C, showing the strong detection and localization of the secondary, with the precisely determined properties tabulated at the upper right, and an assessment (lower right) of the contrast potential of that observation. Courtesy of the NIRISS team.

This has been just a taste of many outstanding performance results obtained during the scientific commissioning of Webb's powerful observing modes. For a more detailed early treatment, we refer once more to Rigby et al. (2022)².

4.4 Stray light features

Though commissioning of Webb's observing modes proceeded remarkably smoothly, it is no surprise that not everything in such a complex, powerful observatory was perfect. The principal unwanted features observed had to do with stray light features of various sorts. We touch on those features here.

Stray light features in two of the instruments, NIRCcam and NIRISS have a similar origin. Termed the NIRCcam “claws” and the NIRISS “light saber”, the features are shown schematically in Figure 17.

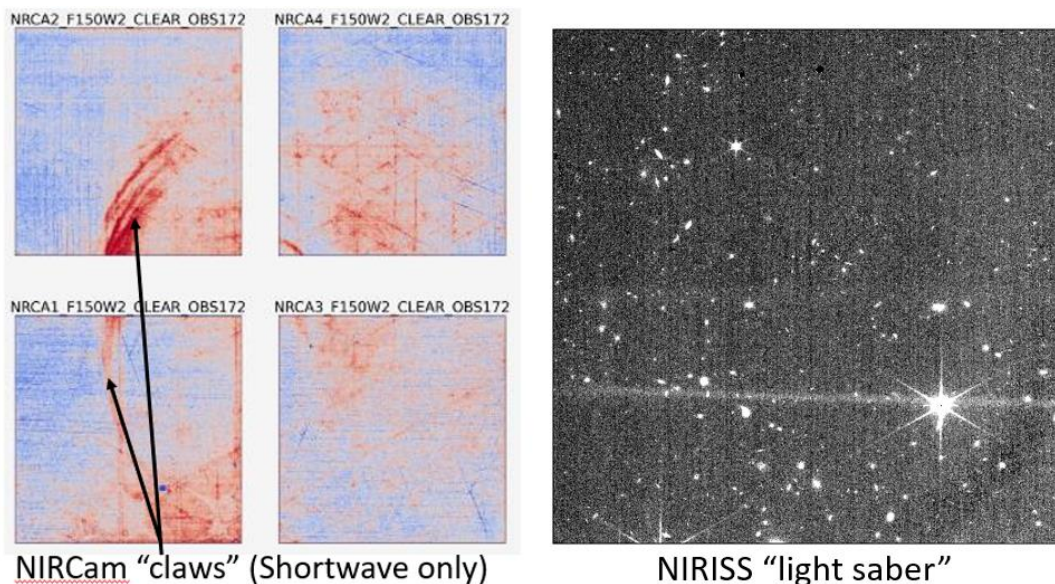


Figure 17. NIRCcam “claws” and NIRISS “light saber”, stray light features with a common origin in the telescope’s “rogue path” (see text). Note that the NIRCcam figure is a highly stretched representation of a sky flat, with sources removed. The cross-hatch features represent actual response differences which belong in the actual flat-field response correction; the arc features highlighted are the pointing-dependent stray light feature. The NIRISS “light saber” is the nearly horizontal bright streak across the detector just above the bright star.

The NIRCcam claws are seen only in the shortwave channel of the instrument (0.6-2.5 μ m); they range up to as high as 15-20% of the zodiacal light brightness and move with changes in pointing direction, but they are not apparent in most pointing directions. The NIRISS light saber ranges from 1-10% and is seen only in that narrow region of the detector. Both of these features have a common origin in the “rogue path” of the observatory. This is a light path that goes directly from a susceptibility region of the sky (of a few square degrees in size), through an aperture mask at the top of the Aft Optical System, straight to the pickoff mirrors of the relevant instrument, without having reflected off *any* of the telescope optics. This path to the pickoff mirrors was recognized early in the mission design, but analyses indicated that there were no direct paths through the instrument *optical* systems to the detectors. Unfortunately, we have found that there are grazing reflection paths off instrument *mechanical* structures that produce the observed features, which are strong only when there is a VERY bright star (brighter than 2nd magnitude or so) in the relevant susceptibility region. The best mitigation therefore is to schedule and orient observations such that this susceptibility region – 10 to 12 degrees away from the actual target – does not contain such bright stars.

There are related, but distinct, stray light features that are termed the NIRCcam “wisps” and the MIRI “glow sticks”. These are indicated in Figure 18.

The “wisp” and “glow stick” features are thought to arise roughly along the same direction as the “rogue path”, but to have undergone a reflection off the underside of one of the Secondary Mirror support struts. The NIRCcam wisps come from sky features reflected along that path; the MIRI features arise from thermal emission from warmer parts of the core region of the observatory. The NIRCcam wisp features vary in brightness but not morphology, and so are amenable to subtraction with a template. The glow sticks made finding the null locations of the 4QPMs more difficult, but once the nulls were found, they have little effect on MIRI coronagraphic performance. They are very steady in brightness and subtract well with a reference image.

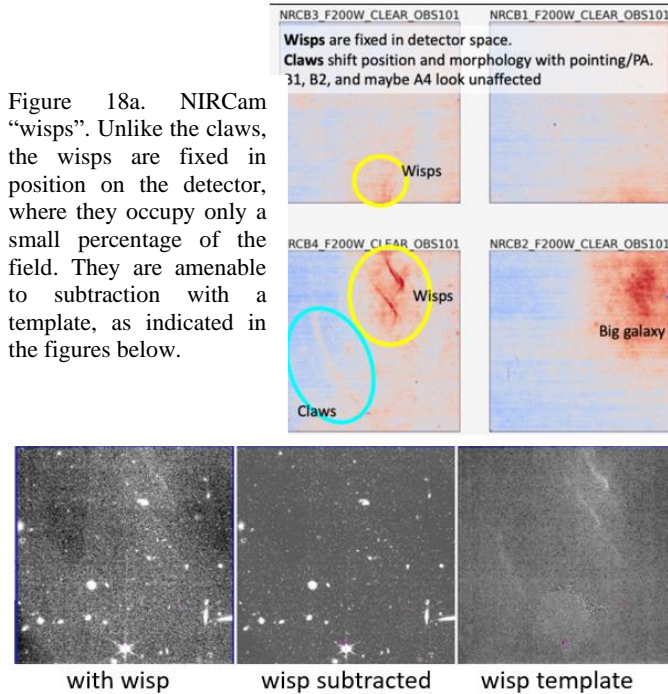


Figure 18a. NIRCam “wisps”. Unlike the claws, the wisps are fixed in position on the detector, where they occupy only a small percentage of the field. They are amenable to subtraction with a template, as indicated in the figures below.

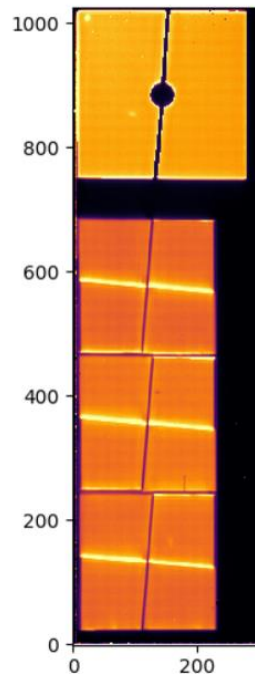


Figure 18b. MIRI “glow sticks”. These features light up the horizontal edges of the focal plane mask that defines the borders of the imager field or Lyot stop (top left) or the horizontal steps of the four-quadrant phase masks (the regions of the three lower squares at the left). This figure shows only the coronagraphic portion of the MIRI imager field – the main imaging field is to the right, not shown.

Further details and mitigation strategies can be found in the JDox web pages under the topic of Data Artifacts and Features. Tools are in development for use within the Astronomer’s Proposal Tool to help observers avoid setting up observations with bright stars in the rogue path susceptibility regions.

5. FINAL RESULTS AND SUMMARY

Though we closed the previous section with a discussion of unwanted stray light features, we emphasize again that the overall performance of the 17 observing modes of Webb’s powerful instrument suite, thoroughly characterized during commissioning, was almost uniformly outstanding. The “science readiness criteria” were nearly always met very comfortably, typically with performance above not only the requirements, but also above the pre-flight expectations, such as derived using the pre-flight Exposure Time Calculator. The ETC will undergo numerous updates, almost always in a favorable direction, before the Cycle 2 Call for Proposals.

Accordingly, the decision meetings regarding mode readiness were quite straightforward. The presentations for the 17 modes took place over a roughly six-week period from June 2nd to July 10th, 2022, starting with NIRCam Imaging and ending with NIRCam coronagraphy. *Every mode was endorsed enthusiastically and approved without hesitation as being ready to support outstanding Cycle 1 science. Each mode offers the astronomical community the exciting new capabilities that the Webb telescope and science instruments were designed to achieve.*

With the technical performance of the modes determined to be excellent, the final focus of the readiness meetings was on any operational liens that would be applicable to particular observations, that observers needed to be alerted to, or that particular observations needed to wait for. These fell into several categories:

- “Good” liens: e.g., warnings to observers that, *due to higher-than-expected throughput* for a given mode, they need to be mindful of earlier-than-expected saturation;
- “Neutral” liens: “normal work” that had not yet been completed, for which specific observations should wait – e.g., waiting for a small software adjustment to the position of a subarray so that it doesn’t clip the edge of a spectrum, or for an update to an astrometric calibration so that the target acquisition process centers the target on a coronagraphic spot more accurately;
- “Warnings”: alerts to observers regarding features like the claws and light saber, with the advice not to set up an observation with exceptionally bright stars in the rogue path susceptibility regions.

During the overlap period between Cycle 1 and commissioning (before the July 12, 2022, Early Release Observation reveal), the data embargo on commissioning results made interacting with the community more challenging. Now that

the commissioning embargo has passed, these communications are much more straightforward. The Rigby et al. (2022)² commissioning performance summary is available, and a great deal of updated documentation in the JDox system at STScI has gone online.

Let us conclude by summarizing the main results of six-plus months of intense commissioning work by hundreds of people:

- The commissioning process of the incredibly complex James Webb Space Telescope – a cryogenic, deployable observatory based a million miles from Earth – went remarkably smoothly.
- The commissioning program left the Observatory in excellent health – all redundant hardware systems are operating on their primary (launch) sides.
- The technical performance of the Observatory is superb, exceeding both requirements and pre-flight expectations.
- The pointing performance and stability exceed requirements.
- The Optical Telescope Element has excellent wavefront error, and the end-to-end combinations of the telescope plus the instruments' optical systems yield sharper images than expected.
- The instruments generally have higher throughput than expected.
- The background levels are equal to or lower than expected.
- As a result of the above, **JWST is more sensitive than expected and will usually go deeper in a shorter time than expected.**
- Time series and high-contrast observing modes are working well “out of the box”.

In all, the outcome of the scientific commissioning of the James Webb Space Telescope has been thrilling, as Webb's powerful new observing capabilities usher in a new era of discovery.

ACKNOWLEDGMENTS

We have noted above the hundreds of people who devoted themselves tirelessly to the grueling Webb commissioning campaign. We wish of course also to acknowledge the *thousands* of people who contributed to the development of JWST over the many years leading up to launch, from NASA, ESA, CSA, and dozens of industrial and educational institutions. It is their efforts that have successfully brought this exciting new tool to the astronomical community and the world.

REFERENCES

- [1] McElwain, M. W. et al., “The James Webb Space Telescope mission status,” Proc. SPIE 12180, in press (2022).
- [2] Rigby, J. et al., “Characterization of JWST science performance from commissioning,” <https://arxiv.org/abs/2207.05632>
- [3] Rieke, M., Kelly, D. and Horner, S., “Overview of James Webb Space Telescope and NIRCams Role,” Proc. SPIE 5904, 1-8 (2005).
- [4] Beichman, C. A., Rieke, M., Eisenstein, D., Greene, T. P., Krist, J., McCarthy, D., Meyer, M., and Stansberry, J., “Science opportunities with the near-IR camera (NIRCam) on the James Webb Space Telescope,” Proc. SPIE 8442, 84422N (2012).
- [5] Jakobsen, P. et al., “The Near-Infrared Spectrograph (NIRSpec) on the James Webb Space Telescope: I. Overview of the instrument and its capabilities,” A&A 661, A80 (2022).
- [6] Ferruit, P. et al., “The Near-Infrared Spectrograph (NIRSpec) on the James Webb Space Telescope: II. Multi-object spectroscopy (MOS),” A&A 661, A81 (2022).
- [7] Böker, T. et al., “The Near-Infrared Spectrograph (NIRSpec) on the James Webb Space Telescope: III. Integral-field spectroscopy,” A&A 661, A82 (2022).
- [8] Birkmann, S. et al., “The Near-Infrared Spectrograph (NIRSpec) on the James Webb Space Telescope: IV. Capabilities and predicted performance for exoplanet characterization,” A&A 661, A83 (2022).
- [9] Rieke, G. H. et al., “The Mid-Infrared Instrument for the James Webb Space Telescope, I: Introduction,” PASP Vol. 127, Issue 953, 584-594 (2015).

- [10] Wright, G. S. et al., “The Mid-Infrared Instrument for the James Webb Space Telescope, II: Design and Build,” *PASP* Vol. 127, Issue 953, 595-611 (2015).
- [11] Doyon, R. et al., “The JWST Fine Guidance Sensor (FGS) and Near-Infrared Imager and Slitless Spectrograph (NIRISS),” *Proc. SPIE* 8442, 84422R (2012).
- [12] Maszkiewicz, M., Saad, K., Rowlands, N., Doyon, R., and Hutchings, J. B., “JWST Fine Guidance Sensor and Near-Infrared Imager and Slitless Spectrograph,” *Optical Payloads for Space Missions* (ed S.-E. Qian), ch35, (2015).
- [13] Feinberg, L. D., Wolf, E., Acton, S., Knight, S., Perrin, M. D., Lallo, M., Reynolds, P., and Keski-Kuha, R., “Commissioning the James Webb Space Telescope Optical Telescope Element,” *Proc. SPIE* 12180, in press (2022).
- [14] Acton, D. S., “Phasing the Webb Telescope,” *Proc. SPIE* 12180, in press (2022).
- [15] Knight, J. S., “Webb telescope imaging performance,” *Proc. SPIE* 12180, in press (2022).
- [16] Birkmann, S. M. et al., “The in-flight noise performance of the JWST/NIRSpec detector system,” *Proc. SPIE* 12180, in press (2022).
- [17] Böker, T. et al., “Status of the JWST/NIRSpec commissioning campaign,” *Proc. SPIE* 12180, in press (2022).
- [18] Giardino, G. et al., “Optical throughput and sensitivity of JWST NIRSpec,” *Proc. SPIE* 12180, in press (2022).
- [19] Lützendorf, N. et al., “Astrometric and wavelength calibration of the NIRSpec instrument commissioning using a model-based approach,” *Proc. SPIE* 12180, in press (2022).
- [20] Dicken, D., Argyriou, I., Garcia-Marin, M., Ressler, M. E., Morrison, J. E., Rieke, G. H., Guillard, P., and Regan, M. W., “Row and column artefacts in JWST MIRI’s Si:As blocked impurity band detectors,” *Proc. SPIE* 12180, in press (2022).
- [21] Bright, S. et al., “JWST MIRI detector characterization: observing modes,” *Proc. SPIE* 12180, in press (2022).
- [22] Girard, J. H. et al., “JWST/NIRCam Coronagraphy: preparing an efficient commissioning with realistic end to end simulations,” *Proc. SPIE* 12180, in press (2022).
- [23] Alves de Oliveira, C. et al., “In-flight performance and calibration of the Grating Wheel Assembly sensors (NIRSpec/JWST),” in *Proc. SPIE* 12180, in press (2022).
- [24] Rawle, T. D. et al., “In-flight performance of the NIRSpec Micro Shutter Array,” *Proc. SPIE* 12180, in press (2022).
- [25] Kutyrev, A. S., Collins, N., Chambers, J., Moseley, S. H., and Rapchun, D., “Microshutter arrays: high contrast programmable field masks for JWST NIRSpec,” *Proc. SPIE* 7010, 70103D (2008).
- [26] Moseley, S. H. et al., “Microshutters arrays for the JWST near-infrared spectrometer,” *Proc. SPIE* 5487, pp. 645-652 (2004).
- [27] Smith, E. C. et al., “On-orbit JWST backgrounds from stray light and thermal emission,” *Proc. SPIE* 12180, in press (2022).